

See discussions, stats, and author profiles for this publication at: <https://www.researchgate.net/publication/272273873>

Functionalization of Carbon Microcoils by Platinum–Loading Through Dendrimer Binder

Article in *Science of Advanced Materials* · January 2013

DOI: 10.1166/sam.2013.1423

CITATIONS

15

READS

51

3 authors, including:



[Ampornphan Siriviriyannun](#)

The Siam Cement Public Company Limited

18 PUBLICATIONS 209 CITATIONS

SEE PROFILE

Functionalization of Carbon Microcoils by Platinum-Loading Through Dendrimer Binder

A. Siriviryanun¹, T. Imae^{1,2,*}, and S. Motojima³

¹Graduate Institute of Applied Science and Technology

²Department of Chemical Engineering, National Taiwan University of Science and Technology,
43 Keelung Road, Section 4, Taipei 10607, Taiwan ROC

³Toyota Physical and Chemical Research Institute, Nagakute, Aichi 480-1192, Japan

ABSTRACT

Pt nanoparticles protected by dendrimers (DEN(PtNP)s) were synthesized and successively covalent-bound to carbon microcoils (CMCs) through amide bonding. DEN(PtNP)s were homogeneously distributed on the surfaces of CMCs at low content of metal precursor. However, as the content of metal precursor was increased, DEN(PtNP)s tended to aggregate on the surfaces of CMCs. Then the content of Pt in composites of CMCs and DEN(PtNP)s increased effectively with the content of metal precursor. It is evident from the absence of a Raman G band that the composites maintain the amorphous character of the CMCs. The electrocatalytic activity toward the methanol oxidation on composite-loaded electrodes was examined, and results of cyclic voltammetry revealed the effective current enhancement with loading CMC/DEN(PtNP)s.

KEYWORDS: Carbon Microcoil, Platinum Nanoparticle, Dendrimer, Raman Spectroscopy, Cyclic Voltammetry, Metal Oxidation.

1. INTRODUCTION

Direct methanol fuel cells (DMFCs) are one of the alternative power sources being developed for vehicles and portable or stationary electronic devices.^{1–3} Major challenge for commercial applications of the DMFCs is the development of stable electrocatalysts with high activities. Pt nanoparticles, (PtNP)s, have been extensively studied as the electrocatalysts for the DMFCs.^{4–6}

Carbon microcoils (CMCs), one of carbon materials, are an amorphous material with 3D-helical structure and high surface area and possess excellent mechanical and electrical properties.⁷ Thus, CMCs could be used as catalyst-supports for the fuel cells. However, since CMCs are indispersed in liquid media, the treatment of CMCs in liquid media is quite difficult. Recently, CMCs have been treated by acid to load carboxylic groups on their surfaces, which have raised the better dispersion of CMCs in water.⁸ Then the functionalized CMCs were immobilized on surface-modified substrates for developing the applications of CMCs to composite devices.^{8,9} In addition, the investigations of the functionalized CMCs were extended to the embedding in a polymer matrix for the reinforcement of film properties,¹⁰ to the composite fabrication with

polyaniline for the electrochemical enhancement,¹¹ and to the template fabrication of hollowed silica microcoils.¹²

In the present work, CMCs functionalized by the acid treatment were upgraded by loading metal (Pt) nanoparticles through dendrimer binder. Thus the chemical immobilization of metal nanoparticles on CMCs could be beneficial for the further development of CMCs in many applications including catalysis and sensing. First, Pt nanoparticles protected by dendrimers (DEN(PtNP)s) were synthesized and then DEN(PtNP)s were covalently immobilized on the CMCs. Successively, the as-prepared composites were immobilized onto the electrodes and their electrocatalytic activity toward the methanol oxidation was then investigated by cyclic voltammetry (CV).

2. EXPERIMENTAL DETAILS

2.1. Materials

CMCs were prepared according to the previously reported procedure.⁷ Amine-terminated fourth generation poly(amido amine) (PAMAM) dendrimer (10 wt% in methanol), Na₂PtCl₆, 1-ethyl-3-(3-dimethylamino-propyl)carbodiimide hydrochloride (EDAC) and 4-mercaptobenzoic acid (MBA) (97%) were products from Aldrich Chemical Co. NaBH₄ was purchased from Wako Pure Chemical Industries Ltd. Sulfuric acid (98%), nitric acid (60%) and ethyl alcohol were commercial

* Author to whom correspondence should be addressed.

Email: imaie@mail.ntust.edu.tw

Received: xx Xxxx xxxx

Accepted: xx Xxxx xxxx

products. Ultrapure water was used on entire experiments. Disposable electrochemical printed (DEP) chips (with screen-printed circular gold (SPCG) or screen-printed circular glassy carbon (SPCGC) working electrode) were purchased from BioDevice Technology, Japan.

2.2. Fabrication of DEN(PtNP)s on Acid-Treated CMCs

Acid-treatment of CMCs was performed according to a previous report.⁸ The mixture of CMCs and HNO₃ was refluxed at 90 °C for 12 h with stirring, and the reaction mixture was filtered through a membrane filter (0.2 μm pore size). Then the filtered residue was washed with water and dried overnight in a vacuum oven at 60 °C.

DEN(PtNP)s were prepared as follows.¹³ An aqueous Na₂PtCl₆ solution was added into an aqueous 0.2 wt% solution of PAMAM dendrimer at various molar ratios (*M:D*) of Na₂PtCl₆ to amine terminal group of dendrimer. The solution of [PtCl₆]²⁻-dendrimer complex was stirred for 3 days, the pH of the solution was adjusted to be 2, and then an aqueous 0.3 M NaOH solution of NaBH₄ (of a 10-fold mole of Na₂PtCl₆) was added to the solution.

Acid-treated CMCs (20 mg) were dispersed in an aqueous DEN(PtNP)s solution (5 cm³) and the dispersion was stirred for 1 h at room temperature. Then the dispersion was added EDC and vigorously stirred for 2 days at room temperature to allow the amide-bond formation. The dispersion was then filtered using a Millipore membrane (PTFE, pore size = 0.2 μm) and the filtered residue was dried overnight at 110 °C.

Self-assembled monolayer (SAM) of carboxyl-terminated thiol on an Au electrode (SAM-SPCG electrode) was fabricated as follows. A SPCG electrode was horizontally immersed into an ethanol solution of MBA (20 mM) for 24 h at room temperature. After that, excess of MBA on the SPCG electrode was removed by rinsing with ethanol and water. Then the SAM-SPCG electrode was dried overnight in a vacuum oven. An aqueous dispersion (10 mg cm⁻³, 10 mm³) of CMC/DEN(PtNP)s was added EDC and retained overnight on the SAM-SPCG electrode to achieve the chemical immobilization of CMC/DEN(PtNP)s on it. The adsorption of the CMC/DEN(PtNP)s on the SPCGC electrode was carried out by dropping a dispersion of CMC/DEN(PtNP)s on the electrode.

2.3. Measurements

Transmission electron microscopic (TEM) images were taken using a Hitachi H-7000 equipped with a CCD camera, operating at a voltage of 100 kV. Specimens for TEM were prepared by dropping sample dispersions onto carbon-coated copper grids and drying in air. Field emission-scanning electron microscopic (FE-SEM) and backscattering SEM images of sample powders on carbon

tapes were performed on a JEOL JSM-6500F operated at a voltage of 20 kV. Thermogravimetric analyses (TGAs) of the powders were performed using a TGA/TA instrument (Perkin Elmer, Q500) under air atmosphere with a heating rate of 10 °C min⁻¹. The infrared (IR) absorption spectra were recorded for powders on an FTIR spectrometer (Nicolet, Nexus 670). Raman spectra were recorded on a Raman microscope (Kaiser Optical Systems) with a laser at an excitation wavelength of 785 nm. The specimens for Raman measurement were fabricated on a glass microfiber filter (Whatman No. 1) by vacuum-filtering and drying overnight at 110 °C. Ultraviolet-visible-near infrared (UV-VIS-NIR) absorption spectroscopic measurements were performed on a Jasco V-670 series UV spectrometer with a 1 mm quartz cell for samples dispersed in ethanol with sonication.

Electrocatalytic activities of CMC/DEN(PtNP)s were evaluated with a Hokuto-Denko HZ-3000 mounted DEP chips. For DEP chips, carbon was served as a counter electrode, Ag/AgCl was served as a reference electrode and gold or glassy carbon was served as a SPCG or SPCGC working electrode, respectively. The working areas of the SPCG and SPCGC electrodes were 3.67 and 2.64 mm², respectively. The chip was supported vertically in a specimen solution (2 cm³) at room temperature to immerse the circular working electrode area. The potential of CV was scanned 20 cycles between -0.2 and 1.2 V at a scan rate of 20 mV s⁻¹. The electrolyte solution was an aqueous 0.5 M H₂SO₄ solution including a 2.0 M CH₃OH. Electrical current densities were calculated by normalizing electrical currents with the working area of the SPCG or SPCGC electrode.

3. RESULTS AND DISCUSSION

DEN(PtNP)s were prepared at five different ratios of Na₂PtCl₆ to amine terminal group of PAMAM dendrimer (*M:D* = 0.1:1, 0.2:1, 0.3:1, 0.4:1 and 0.5:1) at the constant dendrimer concentration (0.2 wt%) as a stabilizer. DEN(PtNP)s were then attached to CMCs by using a condensing agent for binding between amine-terminated groups of the DEN(PtNP)s and carboxyl groups on the surfaces of acid-treated CMCs. The covalent binding was confirmed by the IR absorption spectroscopy, as shown in Figure 1. In the case of acid-treated CMCs, C=O and COO⁻ stretching vibration bands existed at 1722 and 1575 cm⁻¹, respectively. However, the hybrid, CMC/DEN(PtNP)s, displayed a shoulder band of amide I in addition to C=O and COO⁻ bands. This result indicates the remnant of free carboxyl groups on the CMCs after the chemical immobilization of DEN(PtNP)s by amide bond. Since the functional sites were loaded larger amounts on the CMCs than the binding sites of the DEN(PtNP)s, the amide I band attributed to the formation of amide linkage might coexist with the IR bands from residual carboxyl groups.

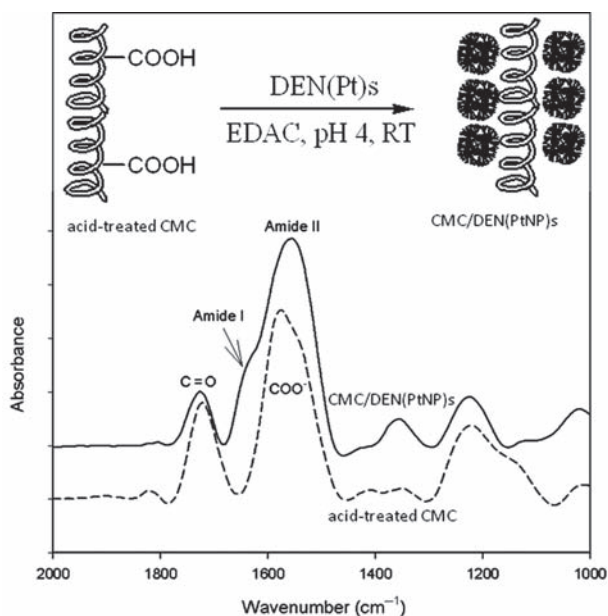


Fig. 1. IR absorption spectra of an acid-treated CMC and CMC/DEN(PtNP)s. Inset is a scheme of the immobilization of DEN(PtNP)s on an acid-treated CMC.

The distribution of DEN(PtNP)s on the CMCs was confirmed with TEM, as shown in Figure 2, where only data of $M:D = 0.1:1$ and $0.4:1$ were represented. It was clearly seen that Pt nanoparticles were successfully fabricated and distributed homogeneously on the CMCs, and the number of Pt nanoparticles increased with $M:D$ ratio (see Fig. 2(b)), in consistency with free DEN(PtNP)s in aqueous dispersions (Fig. 2(c)). It was assumed from TEM at low magnification (Fig. 2(a)) that the surfaces of CMC/DEN(PtNP)s were rougher at high $M:D$ ratios than at low $M:D$ ratios.

The morphology of the hybrid surfaces and the distribution of the Pt nanoparticles on it were preferably clarified from SEM images by using the backscattering secondary electron mode in Figure 3. A FE-SEM image of CMC/DEN(PtNP)s at a $M:D$ ratio = $0.4:1$ in Figure 3(a) is compared with a backscattering SEM image at the same location in Figure 3(b). The bright domains in Figure 3(b) can be attributed to the aggregates of Pt nanoparticles which were immobilized on the surfaces of CMCs. The domains were clear and abundant at high $M:D$ ($0.3:1$ to $0.5:1$) values. Such domains could be observed as depositions on the surfaces of CMCs in Figure 3(c). The tendency on the domain formation of Pt nanoparticles is comparable to the aggregation of DEN(PtNP)s themselves, as seen in Figure 2(c).

The thermal stability of CMC/DEN(PtNP)s was investigated by a TGA under air atmosphere. Figure 4(a) shows TGA curves of an acid-treated CMC and CMC/DEN(PtNP)s. The main degradation temperature of the acid-treated CMC was $655\text{ }^\circ\text{C}$, but that of the CMC/DEN(PtNP)s shifted to the lower temperature with

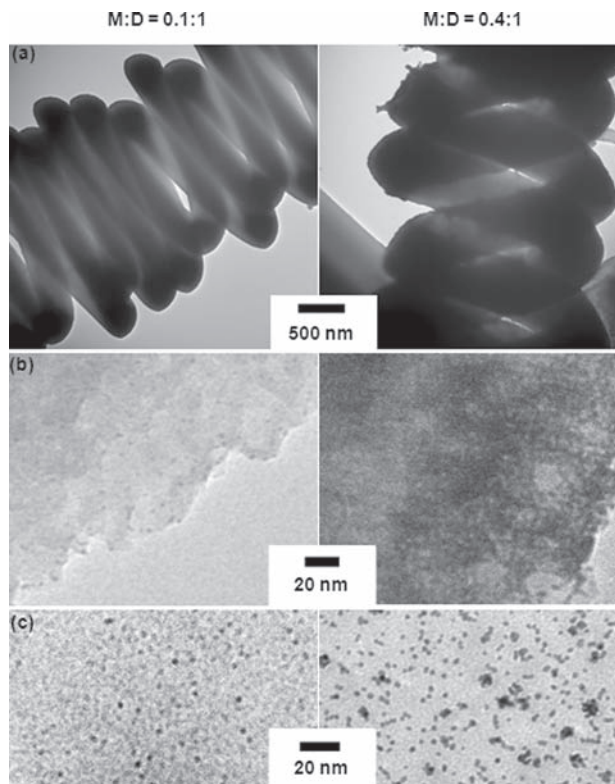


Fig. 2. TEM images of CMC/DEN(PtNP)s and DEN(PtNP)s at $M:D = 0.1:1$ and $0.4:1$. (a), (b) CMC/DEN(PtNP)s, (c) DEN(PtNP)s.

increasing $M:D$ ratio, as plotted in Figure 4(b). It can be assumed that the presence of catalyst, (PtNP)s, can promote the degradation of CMCs in proportion to its amount increasing with $M:D$. Since dendrimers are entirely burnt off up to $400\text{ }^\circ\text{C}$,¹⁴ dendrimers and CMCs are completely vanished at high temperature like $800\text{ }^\circ\text{C}$.

Then the Pt content in hybrids can be quantitatively evaluated from TGA analysis. Since CMCs are synthesized using a metal catalyst,⁷ a small amount of such metal catalysts are mixed in the CMC powders and remain as an ash, even if CMCs were burnt off at high temperature above $700\text{ }^\circ\text{C}$, as seen on a TGA curve of acid-treated CMC in Figure 4(a). Then in order to evaluate the net content of (PtNP)s bound on a CMC, a differential weight loss between acid-treated CMC and CMC/DEN(PtNP)s at $800\text{ }^\circ\text{C}$ was calculated. It can be found from Figure 4(b) that the Pt content in CMC/DEN(PtNP)s increases linearly with $M:D$ ratio up to $9.3\text{ wt}\%$ at $M:D = 0.5:1$.

There were no characteristic absorption bands for CMC/DEN(PtNP)s in the UV-VIS-NIR wavelength region, suggesting no intrinsic electronic absorption of amorphous CMCs. On the other, Raman bands of CMC/DEN(PtNP)s were observed around 1325 and 1600 cm^{-1} , as seen in Figure 5(a). Raman shifts, relative intensities and intensity ratios of these bands are plotted as a function of $M:D$ in Figure 5. It was found that Raman shifts of both bands slightly varied to the lower wavenumber and their relative

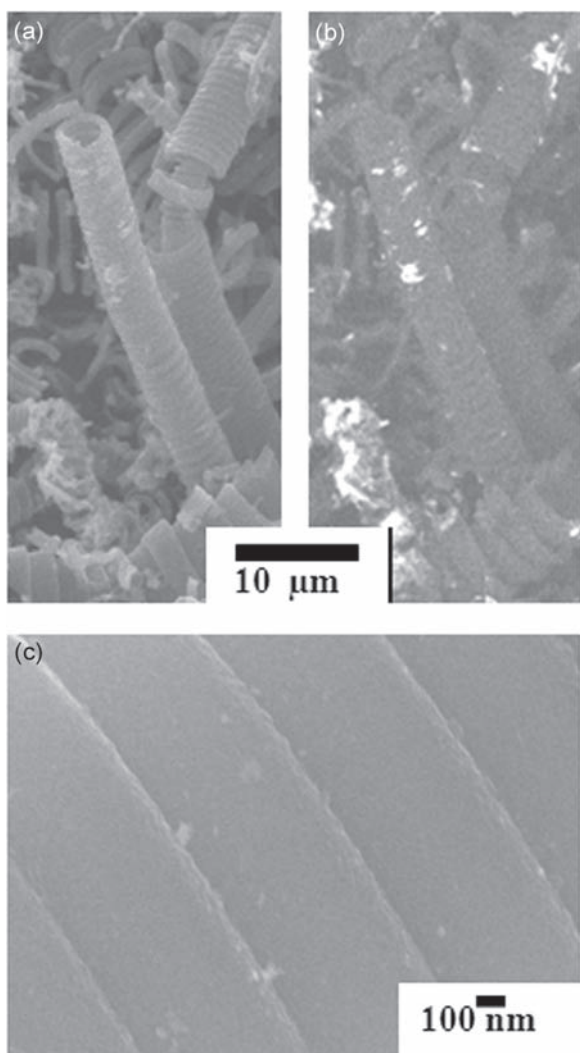


Fig. 3. SEM images of CMC/DEN(PtNP)s at $M:D = 0.4:1$. (a), (c) FE-SEM, (b) backscattering SEM.

intensities increased with increasing $M:D$, although there was no significant variation of the intensity ratios (around 0.8) between two bands. Since these tendencies are similar to those of D and D' bands at 1317 and 1613 cm^{-1} , respectively, but different from that of a G band at 1583 cm^{-1} of carbon nanotubes,^{13, 15, 16} two Raman bands around 1325 and 1600 cm^{-1} of CMC/DEN(PtNP)s can be assigned to D and D' bands, respectively, indicating no G band. This assignment is reasonable, because CMCs are amorphous carbon materials.⁸ This observation is also consistent with the insight from the UV-VIS-NIR absorption spectra as described above.

The electrocatalytic activity of CMC/DEN(PtNP)s toward methanol oxidation was evaluated by a CV. It is apparent from the comparison among CV curves on bare SPCGC, CMC-loaded SPCGC and CMC/DEN(PtNP)s-loaded SPCGC ($M:D = 0.1:1$) electrodes in Figure 6(a) that the current intensity increased with loading CMCs on SPCGC and was enhanced further

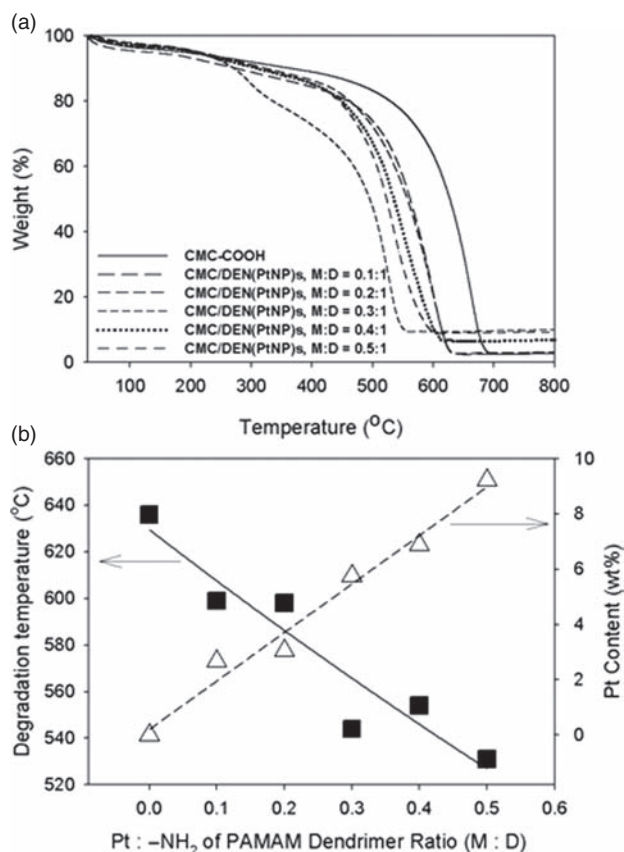


Fig. 4. (a) TGA curves of an acid-treated CMC and CMC/DEN(PtNP)s and (b) plots of degradation temperature and Pt content of CMC/DEN(PtNP)s as a function of $M:D$.

with loading DEN(PtNP)s on CMC-loaded SPCGC. These results indicate the effective influence of CMCs and (PtNP)s on electrocatalytic activity toward methanol oxidation.

The potential and current density of an anodic peak in a CV curve on CMC/DEN(PtNP)s-loaded SPCGC and SAM-SPCG electrodes are plotted as a function of $M:D$ in Figures 6(b) and (c). Anodic peaks of methanol oxidation in the forward scan occurred at 0.26–0.29 and 0.38–0.40 V with current densities of 0.014–0.019 and 0.14–0.19 mA cm^{-2} on SPCGC and SAM-SPCG electrodes, respectively. However, the potential and current density were scarcely or slightly dependent on $M:D$ ratio. The latter results are attributed to enough contribution of (PtNP)s even at $M:D = 0.1:1$ toward methanol oxidation. Meanwhile, the contribution of electrodes is rather remarkable. The lower the potential at the anodic peak, the easier the methanol oxidation occurs on the electrode. Therefore, the CMC/DEN(PtNP)s-loaded SPCGC seems to be more favorable from this standpoint than CMC/DEN(PtNP)s-loaded SAM-SPCG, although the potentials at anodic peak on methanol oxidation by both electrodes are lower than the previous reports.^{5, 17} The former electrode system possesses a shorter electron transfer path from the

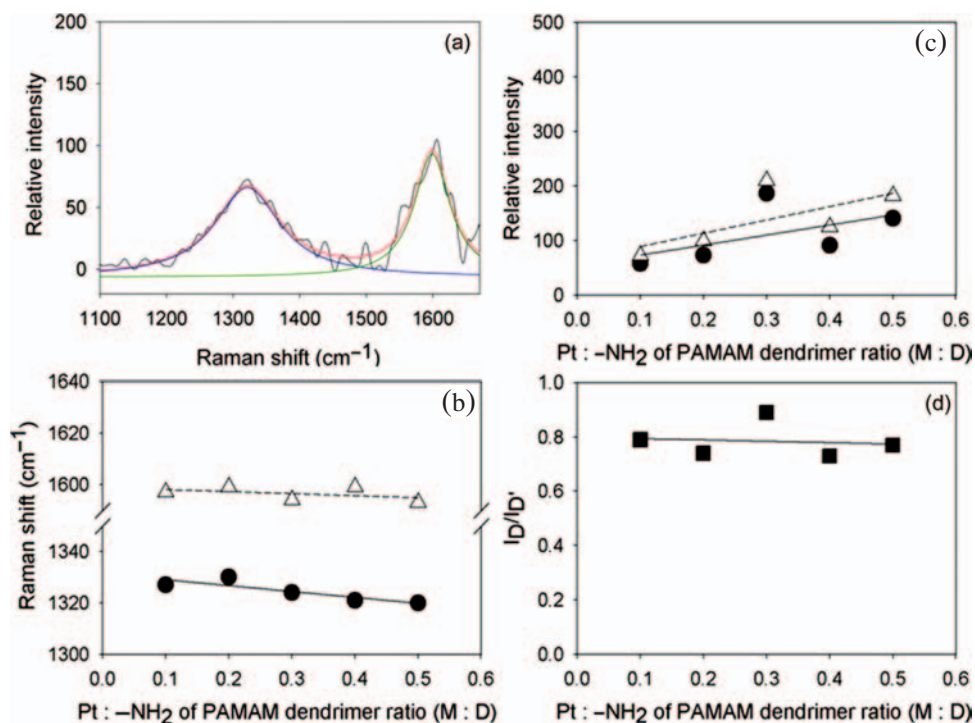


Fig. 5. (a) A Raman Spectrum of CMC/DEN(PtNP)s at $M:D = 0.4:1$ at a excitation wavelength of 785 nm and its deconvolution, (b) Raman shift, (c) relative intensity, and (d) intensity ratio of D and D' bands ($I_D/I_{D'}$) as a function of $M:D$. • D band, Δ D' band.

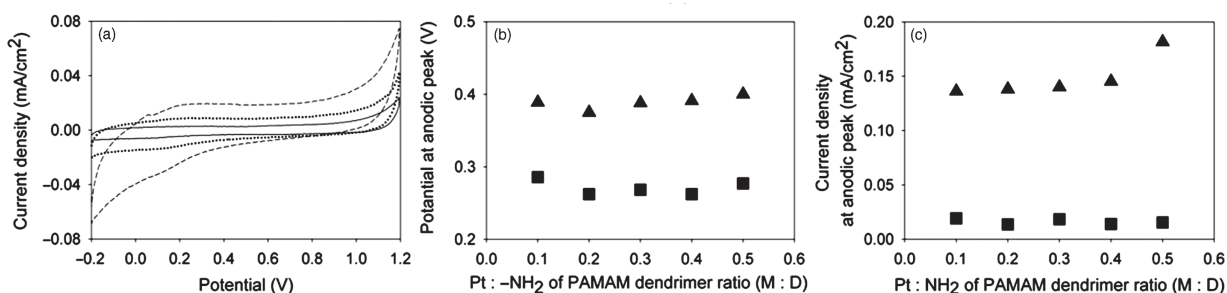


Fig. 6. (a) Cyclic voltammograms on (—) SPCGC, (····) CMC-loaded SPCGC, (---) CMC/DEN(PtNP)s-loaded SPCGC ($M:D = 0.1:1$) electrodes in an aqueous 0.5 M H₂SO₄ solution including a 2 M MeOH. (b) Potential and (c) current density at an anodic peak in cyclic voltammograms on CMC/DEN(PtNP)s-loaded electrodes as a function of $M:D$. Electrode ■: SPCGC, ▲ SAM-SPCG.

catalytic reaction field ((PtNP)s) to the electrode than the latter electrode system, because the SAM exists between CMC/DEN(PtNP)s and electrode. Generally, methanol is oxidized on the surface of PtNPs and carbon dioxide is generated along the following reaction: $\text{CH}_3\text{OH} + \text{H}_2\text{O} \rightarrow \text{CO}_2 + 6\text{H}^+ + 6\text{e}^-$. Thus the current density of an anodic peak in the forward scan should be proportional to the amount of methanol oxidized at the electrode.¹⁸ Then CMC/DEN(PtNP)s-loaded SAM-SPCG electrode is desired, since the current density is one order higher than on CMC/DEN(PtNP)s-loaded SPCGC electrode. CMC/DEN(PtNP)s is preferably loaded on a SAM-SPCG electrode by the chemical immobilization, being different from the load on a SPCGC electrode by the physical adsorption. The more the loading of (PtNP)s is, the more is the catalytic effect.

4. CONCLUSIONS

DEN(PtNP)s were successfully covalent-bound on the surfaces of CMCs. It was found that DEN(PtNP)s were homogeneously immobilized on CMCs at low $M:D$ values like 0.1:1 and 0.2:1. However, as the $M:D$ ratio increased up to 0.5:1, DEN(PtNP)s tended to aggregate on the surfaces of CMCs. Additionally, the immobilization of DEN(PtNP)s affected the thermal stability of CMCs, as the decomposition of the composites occurred at the lower temperature owing to the catalytic effect of (PtNP)s that increases with $M:D$. These tendencies are similar to those of composites of carbon nanotubes with DEN(PtNP)s.¹³ Meanwhile, different from carbon nanotubes,¹³ amorphous characters of the CMCs were maintained because of the absence of a Raman G band in the composites.

In addition, CMC/DEN(PtNP)s were successfully loaded on SPCGC and SAM-SPCG electrodes through adhesion and chemical bindings, respectively. (PtNP)s have a role of a catalyst on the electrochemistry, CMCs are a holder of (PtNP)s and dendrimers behave as a protector of (PtNP)s, a binder between (PtNP)s and an electrode, and a holder of a redox compound. The loading of CMC/DEN(PtNP)s on the SAM-SPCG electrode enlarged the current density toward methanol oxidation, because of large amounts of loading of (PtNP)s, indicating the enhancement of the electrocatalytic efficiency by the aid of CMC and dendrimer. These results suggest the effective application of these composites and composite-loaded electrodes as functional materials and electrocatalytic devices.

Acknowledgments: This subject was financially supported by National Science Council, Taiwan, and Department of Science and Technology, India, for research funding within the frame of the bilateral cooperation programs (NSC 99-2923-M-011-002-MY3). A. Siriviriyannun gratefully acknowledges National Taiwan University of Science and Technology, Taiwan, for the financial support by Postdoctoral Fellowship. We thank Professor B. Huang of National Taiwan University of Science and Technology, Taiwan, for his kind permission of the use of a Raman Instrument.

References and Notes

1. A. S. Arico, S. Srinivasan, and V. Antonucci, *Fuel Cells* 1, 133 (2001).
2. Z. Liu, X. Y. Ling, B. Guo, L. Hong, and J. Y. Lee, *J. Power Sources* 167, 272 (2007).
3. S. Liu, W. Yu, C. Chen, A. Lo, B. Hwang, S. Chien, and S. Liu, *Chem. Mater.* 20, 1622 (2008).
4. J. Huang, Z. Liu, C. He, and L. M. Gan, *J. Phys. Chem. B* 109, 16644 (2005).
5. Y. J. Gu and W. T. Wong, *Langmuir* 22, 11447 (2006).
6. P. Yu, Q. Qian, Y. Lin, and L. Mao, *J. Phys. Chem. C* 114, 3575 (2010).
7. S. Motojima and X. Chen, *Bull. Chem. Soc. Jpn.* 80, 449 (2007).
8. D. P. Adhikari, Y. Tai, M. Ujihara, C. C. Chu, T. Imae, and S. Motojima, *J. Nanosci. Nanotech.* 10, 833 (2010).
9. D. P. Adhikari, T. Imae, and S. Motojima, *Chemical Engineering J.* 174, 693 (2011).
10. D. P. Adhikari, M. Ujihara, T. Imae, P. D. Hong, and S. Motojima, *J. Nanosci. Nanotech.* 11, 1004 (2011).
11. I. Shown, T. Imae, and S. Motojima, *Chemical Engineering J.* 187, 380 (2012).
12. C. Rodriguez-Abreu, N. Vilanova, C. Solans, M. Ujihara, T. Imae, A. Lopez-Quintela, and S. Motojima, *Nanoscale Research Letters* 6, 330 (2011).
13. A. Siriviriyannun and T. Imae, *Phys. Chem. Chem. Phys.* 14, 10622 (2012).
14. X. Lu and T. Imae, *J. Phys. Chem. C* 111, 2416 (2007).
15. X. Zhao and Y. Ando, *Jpn. J. Appl. Phys.* 37, 4846 (1998).
16. S. Ju, J. M. Lee, Y. Jung, E. Lee, W. Lee, and S. J. Kim, *Sensors and Actuators B: Chemical* 146, 122 (2010).
17. D. J. Guo and S. K. Cui, *J. Solid State Electrochem.* 12, 1393 (2008).
18. L. Dong, R. R. S. Gari, Z. Li, M. M. Craig, and S. Hou, *Carbon* 48, 781 (2010).